

An Object Detecting Signal Analysis Method Based on General Approximation Entropy and Wavelet De-noising

Zhenzhong Shen¹, Zhan Zhang¹, Juncai Xu^{1*}, Xin Xie², Zhengyu Yang²

1.College of Water Conservancy and Hydropower Engineering, Hohai University, Nanjing, China

2.Department of Electrical and Computer Engineering, Northeastern University, Boston, USA

*Corresponding author

E-mail: zhzhshen@hhu.edu.cn, zhanzhang_hhu@qq.com, xujc@hhu.edu.cn, xie.x@husky.neu.edu, yang.zhe@husky.neu.edu

Abstract

The construction quality of the bolt is directly related to the safety of the project. The construction quality of the bolt anchorage must be tested. In this paper, the improved complete ensemble empirical mode decomposition (ICEEMD) method is introduced into the bolt detection signal analysis. The ICEEMD is used to decompose the anchor detection signal according to the approximate entropy of each intrinsic mode function (IMF). The noise of the IMFs is eliminated by the wavelet soft threshold de-noising technique. Based on the approximate entropy and the wavelet de-noising principle, the ICEEMD-De anchor signal analysis method is proposed. From the analysis of the vibration analog signal, as well as the bolt detection signal, the result shows that the ICEEMD-De method is able to correctly separate the different IMFs under the noisy condition, and the IMF can effectively identify the reflection signal of the end of the bolt.

Keywords: bolt anchorage, approximate entropy, wavelet de-noise, ICEEMD

1. Introduction

The bolt anchoring system is subject to the geological conditions and the construction technology effect. If there are any hidden dangers that haven't been detected, it will cause engineering accidents and serious economic losses. Therefore, the construction quality of the bolt anchorage must be checked in order to ensure the safety of the project. During the early stage, the detection of the anchor's anchoring quality is mainly based on the drawing test^[1, 2]. However, the method will cause the damage of the anchoring system. The method is also not suitable for large-scale detection and can't be fully reflected^[3].

The detection method of the anchor quality will be gradually replaced by the use of non-destructive testing methods, such as the acoustic wave method^[4, 5]. This method is established based on the mathematical model of the one-dimensional elastic rod^[6]. The assumption is that the longitudinal wave wavelength that is generated by the exciting force is much larger than that of the bolt radius, so the transverse displacement of the system can be neglected. By solving the longitudinal one-dimensional wave equation, the dynamic response of the bolt system is obtained.

The low-end reflection signal of the bolt is easily disturbed during the process of bolt

detection. It is difficult to directly obtain the reflected wave arrival time. In order to obtain the effective signal, many data processing methods, such as the short-time Fourier transform, the Gabor transform, the Wigner-Ville transform, the wavelet transform and so on, are proposed. Wavelet transform is the most used signal analysis method among them^[7-10]. However, the effect of the wavelet transform is often limited by the wavelet base, as well as the number of decomposed layers.

The empirical mode decomposition (EMD) can adaptively select the substrate according to the characteristics of the signal for the multi-resolution analysis of the signal, and overcome the wavelet base selection problem^[11]. However, the EMD has modal aliasing problems during the processing procedure. The Ensemble empirical mode decomposition (EEMD) overcomes the modal aliasing problem that's inherent of the EMD^[12], but because of the addition of different white noise, the decomposition may produce a false mode, which also causes errors. In recent years, the improved complete EEMD (ICEEMD) has been proposed by adding adaptive white noise to the signal and by redefining the calculations of the local mean for each model^[13, 14]. The result shows that the method is superior to the traditional method. However, the actual signal is under noise interference. The processing signal under noise is critical problem with ICEEMD for bolt detection.

Based on the mentioned research, the ICEEMD method was introduced into the bolt detection signal analysis in this paper. By combining the approximate entropy and the wavelet de-noising principle, the ICEEMD-De was established based on the ICEEMD. Then, the ICEEMD-de was used to process the simulation vibration signal and the actual bolt detection signal.

2. Theory and Methodology

Based on the ICEEMD anchor detection signal analysis method, the ICEEMD-De integrates the approximate entropy and wavelet de-noising. The method takes the approximate entropy as the condition of whether the IMF is de-noised. By means of the wavelet soft threshold de-noising technique, the noise in the intrinsic mode function (IMF) is eliminated. The original signal components are retained in maximum; the ICEEMD-De analysis process is shown in Figure 1.

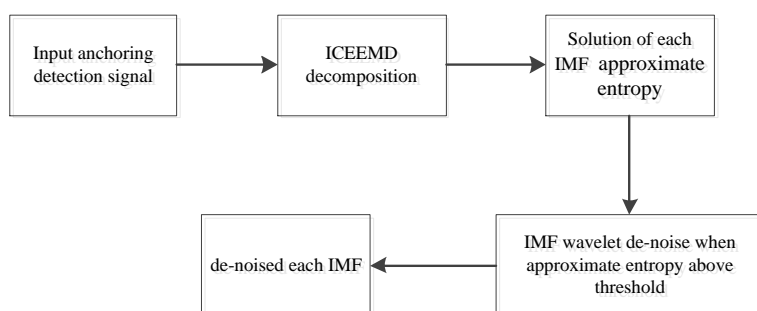


Fig.1. Anchoring detection signal analysis flowchart using ICEEMD-De.

2.1. ICEEMD Principle

The ICEEMD method is able to effectively prevent the occurrence of false IMF by adding the adaptive white noise to the signal and by redefining the local mean of each modal. Assuming the anchor detection signal s , then the decomposition process of the ICEEMD is as follows:

1) The signal s is added to the M group Gaussian white noise in order to generate a new signal s^i . s^i can be expressed as:

$$s^i = s + \beta_k w^i \quad (1)$$

Where $w^i(i=1,2,\dots,M)$ is one group of Gaussian white noise, $\beta_k = \varepsilon_0 \text{std}(r_k)$, r_k is the k -th residue, ε_0 takes 0.2.

2) The k -th mode can be obtained by EMD. We can obtain the mean of the k -th mode and have:

$$\langle E_k(s^i) \rangle = s^i - \langle M(s^i) \rangle \quad (2)$$

where $\langle \rangle$ is the operator of mean.

3) s^i is decomposed by using EMD. We obtain 1-th residue r_1 and 1-st IMF d_1 . We have:

$$r_1 = \langle M(s^i) \rangle \quad (3)$$

$$d_1 = s - r_1 \quad (4)$$

4) We take 2-nd residue, r_2 , as the local mean of $r_1 + \beta_1 E_2(w^i)$. The 2-nd IMF d_2 is:

$$r_2 = \langle M(r_1 + \beta_1 E_2(w^i)) \rangle \quad (5)$$

$$d_2 = r_1 - r_2 \quad (6)$$

5) For any r_k , and k -th IMF d_k , the expression is as follows:

$$r_k = \langle M(r_{k-1} + \beta_{k-1} E_k(w^i)) \rangle \quad (7)$$

$$d_k = r_{k-1} - r_k \quad (8)$$

Go to step 3), we obtain all of the IMF.

2.2. Approximate Entropy

All of the IMF approximate entropy can be expressed as $\{A\} = \{A_1, A_2, \dots, A_k\}$. Then

the calculation procedure A_k is as follows:

1) Take k -th IMF as the time series of n points and define it as:

$$\{Z\} = \{z_1, z_2, \dots, z_n\} \quad (9)$$

2) Compute the binary distance matrix B of the time series:

$$B = \begin{bmatrix} b_{11} & b_{11} & \cdots & b_{1n} \\ b_{21} & b_{22} & \cdots & b_{2n} \\ \vdots & \vdots & & \vdots \\ b_{n1} & b_{n2} & \cdots & b_{nm} \end{bmatrix} \quad (10)$$

where $b_{ij} = \begin{cases} 1, & |z_i - z_j| < a \\ 0, & |z_i - z_j| \geq a \end{cases}$, a is threshold.

3) Compute the ratio of $n+m+1$ and $n-m+2$ to number for B matrix element less than $a C_i^2$

and C_i^3 is as following:

$$C_i^2 = \sum b_{ij} \cap b_{(i+1)(j+1)}, j = 1, 2, \dots, n-1 \quad (11)$$

$$C_i^3 = \sum b_{ij} \cap b_{(i+1)(j+1)} \cap b_{(i+2)(j+2)}, j = 1, 2, \dots, n-2 \quad (12)$$

4) Compute the C_i of the nature logarithm, and get the average of the C_i of the nature logarithm. Then the approximate entropy of the k -th IMF A_k is as follows:

$$\Phi_1 = \frac{1}{n-m+1} \sum_{i=1}^{n-m+1} \ln C_i^2 \quad (13)$$

$$\Phi_2 = \frac{1}{n-m+2} \sum_{i=1}^{n-m+1} \ln C_i^3 \quad (14)$$

$$A_k = \Phi_1 - \Phi_2 \quad (15)$$

5) The wavelet de-noise is performed with the approximate entropy of the IMF greater than the threshold.

2.3. Wavelet De-noise

The wavelet de-noise is achieved based on a critical threshold. The main steps of its de-noise principle are as follows:

1) Select the appropriate wavelet base and the number of decomposition layers. We take the wavelet transform with the noise signal s and obtain its wavelet coefficients w^j :

$$v^{j-1} = D_0 H v^j \quad (16)$$

$$w^{j-1} = D_0 G v^j \quad (17)$$

Where H is the low-pass filter, G is the high-pass filter, v is for the scale factor, and w is the wavelet coefficient.

2) Select the appropriate threshold function to process the wavelet coefficients w^j and get the estimation wavelet coefficients \hat{w}^j :

$$\begin{cases} \hat{w}^j = \text{sgn}(w^j)(|w^j| - \lambda), & |w^j| \geq \lambda \\ \hat{w}^j = 0, & |w^j| \leq \lambda \end{cases} \quad (18)$$

where λ is threshold.

3) use the estimation wavelet coefficients \hat{w}^j and get the reconstruct signal \hat{v}

$$\hat{v}^j = \tilde{H}U\hat{w}^{j-1} + \tilde{G}Uv^{j-1} \quad (19)$$

where \tilde{H} is reconstruct low-pass filter, \tilde{G} is reconstruct high-pass filter.

3. Vibration Simulation Signal Analysis

Focusing on the analysis of the anchor detection signal, one vibration simulation signal is considered, and the signal is decomposed by means of ICEEMD. The ICEEMD method is used in order to analyze the signal under the noise interference condition. The noise signal is directly decomposed by the ICEEMD, ICEEMD decomposition after the wavelet de-noising and ICEEMD-De for studying processing effect.

3.1. Vibration Signal Decompose with ICEEMD

The supposed vibration simulation signal s is composed of the s_1 and s_2 two sine function (Fig.2.). The expression is as follows:

$$s_1 = \sin(20\pi t) \quad (20)$$

$$s_2 = \begin{cases} 0.4 \times \sin(100\pi t) & \text{when } 0.15 \leq t \leq 0.25 \\ 0 & \text{other} \end{cases} \quad (21)$$

$$s = s_1 + s_2 \quad (22)$$

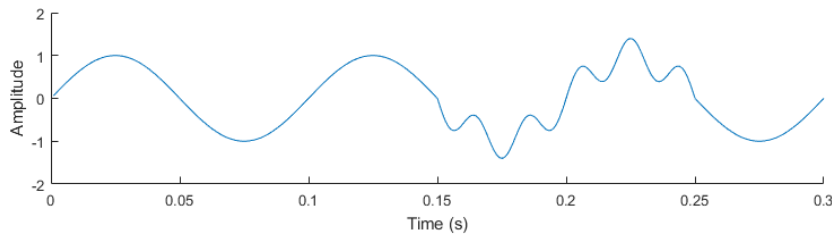


Fig.2. Vibration simulation synthetic signal.

The simulation synthetic signal in Fig.2 is decomposed with the ICEEMD. The analysis results in Fig.3 show:

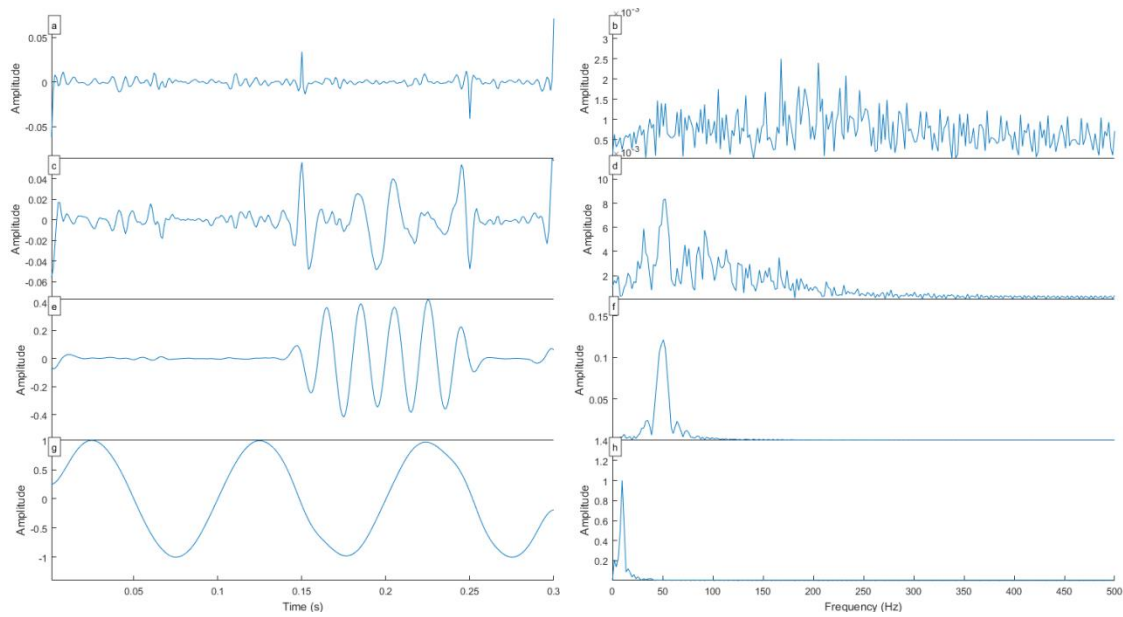


Fig.3. IMF and spectrum after the decomposition of the vibration signal with ICEEMD: Fig.3 (a) (c) (e) (g)IMF1 ~ IMF4. Fig3. (b) (d) (f) (h) IMF4 spectrum.

According to Fig. 3, the ICEEMD decomposes the s signal into four different IMFs, where the latter two characteristic moduli correspond to s_2 and s_1 , respectively, with the corresponding frequencies of the IMF being clearly seen according to the spectrum. Fig 3(b) (d) shows the frequency of both s_2 and s_1 , which are 100Hz and 20Hz, respectively. Fig 3(b) (d) shows that the IMF1 and the IMF2 are mainly high frequency noise signals.

3.2. Vibration Signal Mode Decomposition under Noise Condition with ICEEMD

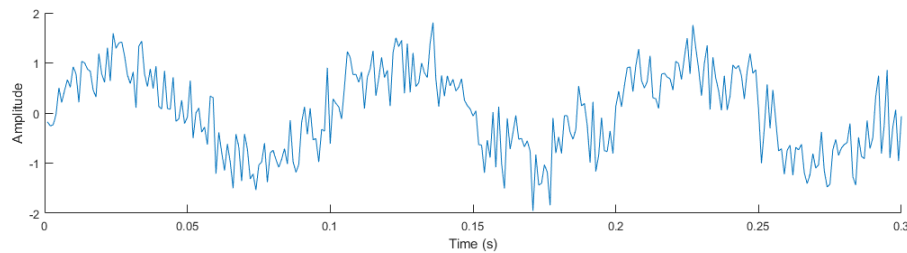


Fig.4. Vibration signal under noise condition.

The random signal is added to the source signal in Fig. 2. We take SNR=5dB as example for the analysis. The signal at 5dB is analyzed by means of ICEEMD and ICEEMD-De. The results are shown in Fig.5 and Fig.6.

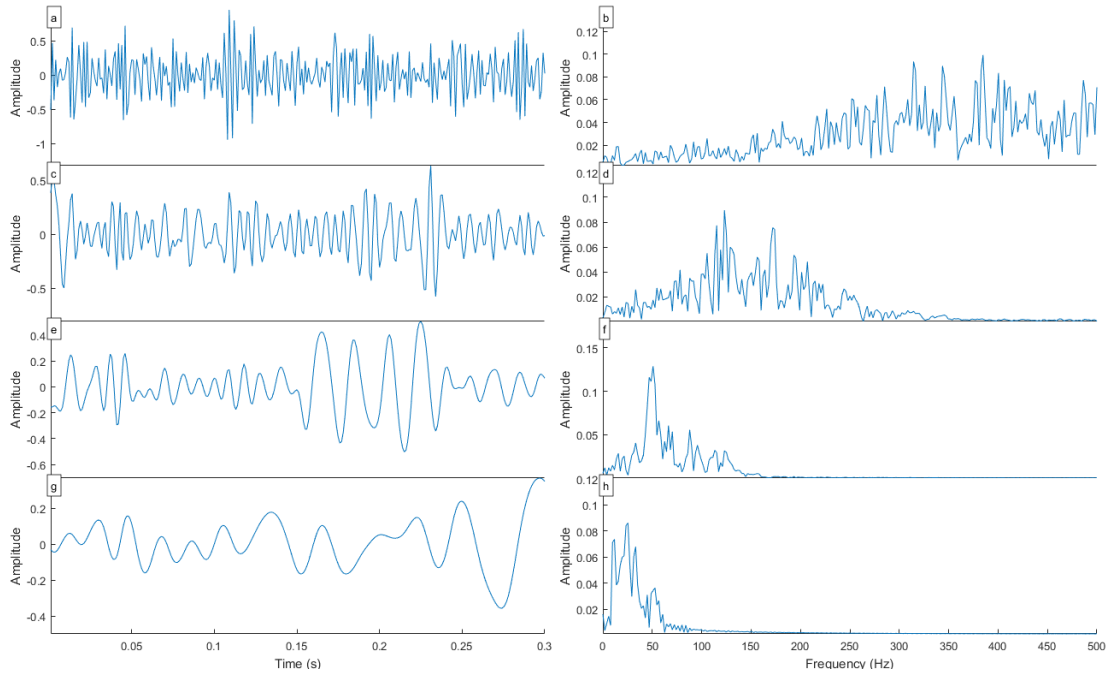


Fig.5. The IMF and spectrum which the vibration signal after the decomposition with ICEEMD: Fig.5 (a) (c) (e) (g) is IMF1 ~ IMF4 and Fig.5 (b) (d) (f) (h) is IMF1~IMF4 spectrum.

According to Fig. 5, the IMF1 and IMF2, which were decomposed by ICEEMD, are still dominated by the random noise signal, while the IMF3, 4 corresponding s_1 and s_2 are doped with a large number of random interference components.

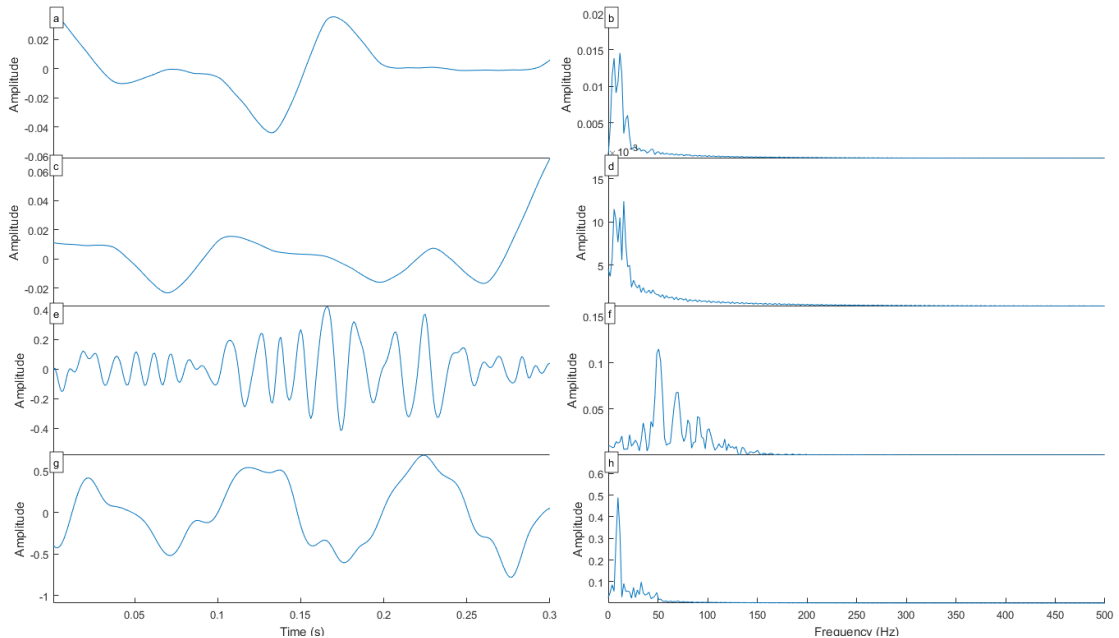


Fig.6.The IMF and spectrum which the vibration signal after the decomposition with ICEEMD-De: Fig.5 (a) (c) (e) (g) is IMF1 ~ IMF4 and Fig.5 (b) (d) (f) (h) is IMF1~IMF4 spectrum.

From Fig. 6, it can be seen that a large number of random noise interference in IMF1,2 has removed, and the IMF3,4 corresponding s_1 , s_2 , which components of the interference

were significantly suppressed. The de-noise signal can clearly distinguish between the s1, s2 frequency of 100Hz and 20Hz.

In order to further study the effect of the proposed method on the de-noising of the vibration signal, the de-noising effect of the wavelet and the ICEEMD-De method on the s signal is compared. Fig. 7 shows the error of the vibration signal after the treatment.

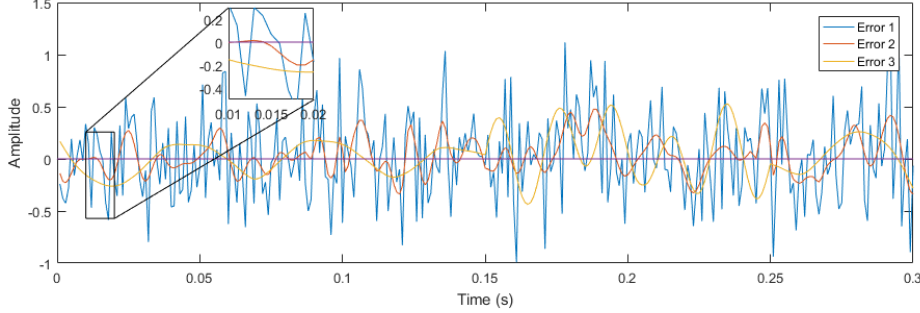


Fig 7. De-noising error line with Wavelet and ICEEMD-De

In Fig. 7, Error1 is the noise error, Error2 is the error after the ICEEMD de-noising and Error3 is the error after the wavelet de-noising. From Fig.7, it can be seen that both methods are able to significantly reduce the noise interference. Based on the general trend of the error line, the proposed method results in the error line frequency being higher, but the error size is lower than the wavelet de-noising.

In the signal de-noising analysis, the signal-to-noise ratio (*SNR*) and the root-mean-square deviation (*RMSE*) are used to measure the de-noising effect of the signal, which is defined as follows:

$$SNR = 10 \lg \left\{ \frac{\sum_{i=1}^N X_i^2}{\sum_{i=1}^N (X - \hat{X}_i)^2} \right\} \quad (23)$$

$$RMSE = \sqrt{\frac{\sum_{n=1}^N (X_i - \hat{X}_i)^2}{N}} \quad (24)$$

According to the formulas(23) (24), two different methods can be calculated in order to de-noise the effect of the index. The index is shown in Table 1.

Table.1. ICEEMD de-noising performance index

Index	Original signal	ICEEMD	Wavelet
SNR (dB)	5.000	13.741	11.179
RMSE	0.411	0.151	0.201

From Table 1, we can see that the two methods are able to greatly improve the *SNR* of the original signal, which is consistent with the results that are shown in Fig 7. The proposed method improves the *SNR* of the original signal 2.7 times, while the Wavelet method increases the *SNR* of the original signal 2.2 times. The proposed method's *RMSE* is smaller than the Wavelet method. Therefore, the ICEEMD-De de-noising effect is superior to that of the Wavelet de-noising method.

4. Analysis of Bolt Detection Signals

Taking the high-slope anchor grouting test of Yunnan-highway as an example, the instrument is the LX-10 bolt, the sampling frequency is 10498Hz, the sampling point is 980 and the sampling interval is 4.0us. The collected vibration signal is shown below in Fig 8.

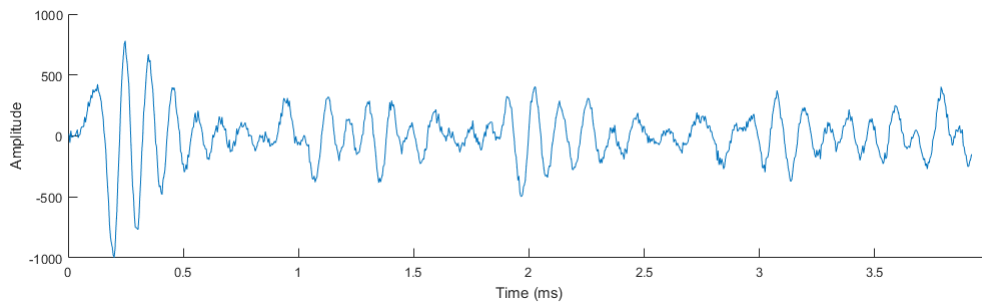


Fig.8.Bolt detection signal in actual engineering

The anchor detection signals in Fig. 8 are decomposed by the ICEEMD method and ICEEMD-De, respectively. The results are shown in Fig. 9 and Fig. 10.

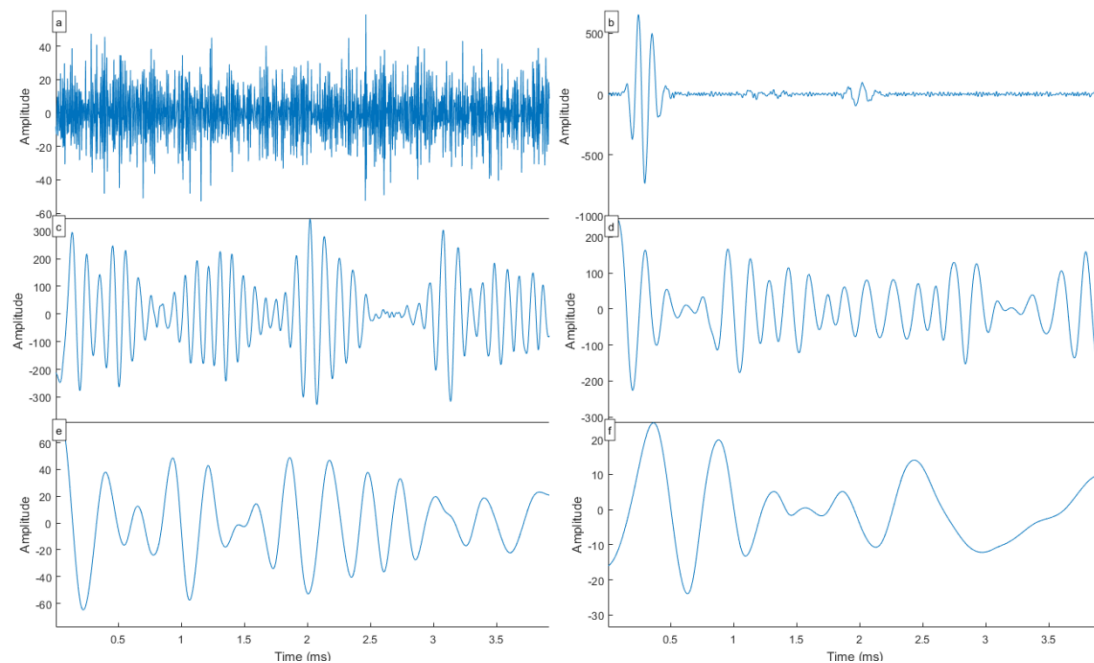


Fig.9. Fig.9 (a) ~ (f) show IMF1 ~ 6 Signal decomposed with ICEEMD.

According to Fig.9, the IMF1 presents in the high frequency noise signal, and the frequency of the IMF1 ~ 6 vibration modes gradually increases. In the modal IMF2, it is obvious that the noise signal can be seen. At 1.1ms, in the background of the bottom of the anchor reflection, the signal can be identified; however, the characteristics are not clear enough.

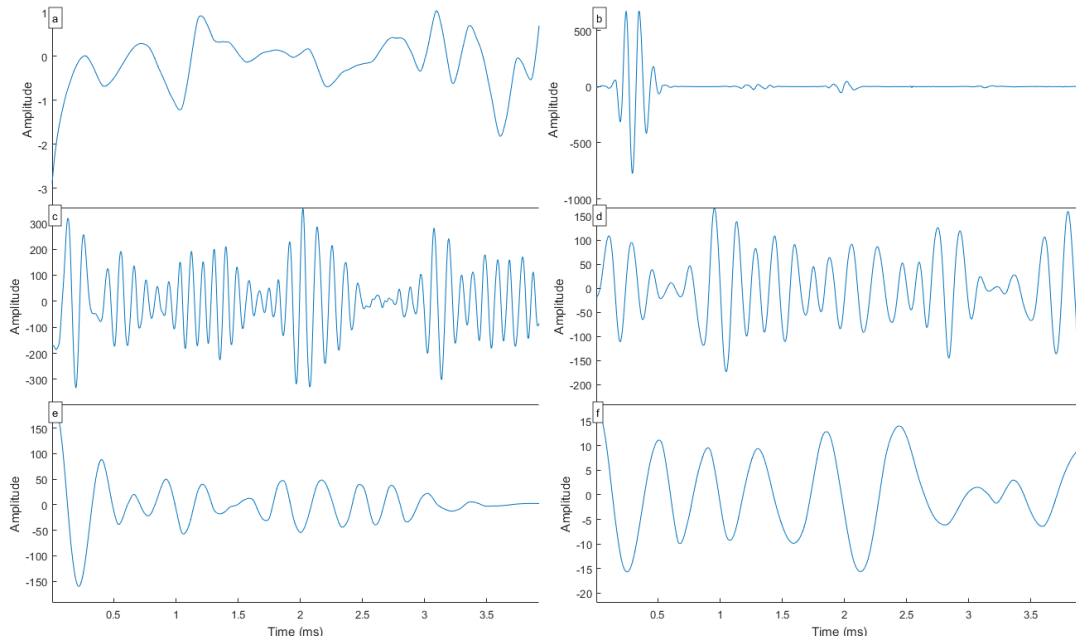


Fig. 10. (a)~(f) shows t IMF1 ~ 6 which is the signal decomposed with ICEEMD-De.

According to Fig. 10, the noise signal in each of the modes is obviously suppressed, with the frequency of the IMF1 ~ 6, the vibration modes gradually decrease, and the reflection signal of the bottom of the bolt becomes clear at 1.1ms in the modal IMF2. Fig.11 shows the initial reflection at 1.1ms in Zoom mode, and noise interference signal was significantly suppressed. As such, the de-noising effect is obvious.

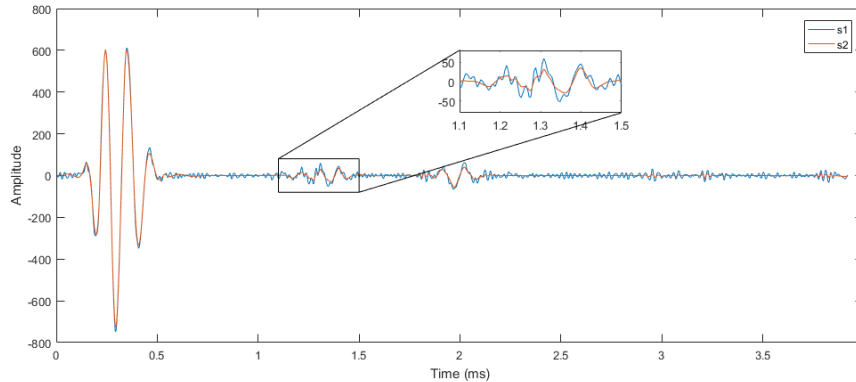


Fig. 11. ICEEMD IMF2vs. ICEEMD-De IMF2

5. Conclusions

Based on the principle of the ICEEMD decomposition, the general approximation entropy and wavelet de-noising, the ICEEMD method is introduced into the bolt detection signal analysis. The anchor detection signal is decomposed by means of using the ICEEMD, while the approximate entropy is regarded as the condition for whether or not the IMF is de-noising. Using the wavelet soft threshold de-noising technique eliminates the noise in the IMF. The ICEEMD-De anchor signal analysis method is proposed. Based on the usage of the ICEEMD-De to analyze the vibration's analog signal and the anchor detection signal, the following conclusions are drawn:

- 1) The ICEEMD method can effectively separate the vibration modal signals to IMF.
- 2) The ICEEMD-De method can effectively remove the interference in the vibration

detection signal, and the de-noising effect is superior to that of the traditional Wavelet method.

3) The ICEEMD method is able to separate each IMF from the bolt detection signal, and the IMF can effectively identify the bolt end reflection time.

4) In the analysis of the bolt detection signal, the ICEEMD-De is more effective for suppression of the the interference than the ICEEMD is.

Acknowledgments

This research was funded by the Open Research Fund of the Fundamental Science on Radioactive Geology and Exploration Technology Laboratory (Grant No.RGET1502) and A Project Funded by the Priority Academic Program Development of Jiangsu Higher Education Institutions (Grant No.3014-SYS1401). The author wish to thank the Su Jiankun from Yunnan Aerospace Engineering Geophysical Limited by Share Ltd for providing the GPR practical detection data used in this study.

References

- Stimpson B. A simple rock bolt pull-out test device for teaching purposes[J]. *International Journal of Rock Mechanics & Mining Sciences & Geomechanics Abstracts*. 1984, 21(4): 217-218.
- Shuan-Cheng G U, Zhang J, Zhang S, et al. Influence Analysis of Anchoring Defects on Bolt Pull-out Load[J]. *Safety in Coal Mines*. 2013.
- Beard M D, Lowe M J S. Non-destructive testing of rock bolts using guided ultrasonic waves[J]. *International Journal of Rock Mechanics & Mining Sciences*. 2003, 40(4): 527-536.
- Song G, Li W, Wang B, et al. A Review of Rock Bolt Monitoring Using Smart Sensors[J]. *Sensors*. 2017, 17(4).
- Zhang J Q, Ji-Min W U, Peng G, et al. Factors in quality of special bolts based on sonic non-destructive detection[J]. *Journal of Hohai University*. 2009, 37(2): 179-184.
- Wang G, Li B. Research on Non-destructive Testing Techniques of Bolt[J]. *Chinese Journal of Engineering Geophysics*. 2009.
- Wang J Y, Zhao Y C, Yao B H, et al. Filtering detecting signal of rockbolt with harmonic wavelet[J]. *International Journal of Mining Science and Technology(矿业科学技术学报)*. 2010, 20(3): 411-414.
- Lee I M, Han S I, Kim H J, et al. Evaluation of rock bolt integrity using Fourier and wavelet transforms[J]. *Tunnelling & Underground Space Technology Incorporating Trenchless Technology Research*. 2012, 28(28): 304-314.
- Szmajda M, Górecki K, Mroczka J. Gabor Transform, SPWVD, Gabor-Wigner Transform and Wavelet Transform - Tools For Power Quality Monitoring[J]. *Metrology & Measurement Systems*. 2010, 17(3): 383-396.
- Xu J, Ren Q, Shen Z. Low strain pile testing based on synchrosqueezing wavelet transformation analysis[J]. *JOURNAL OF VIBROENGINEERING*. 2016, 18(2): 813-825.
- Huang N E, Wu Z. A review on Hilbert-Huang transform: Method and its applications to geophysical studies[J]. *Reviews of Geophysics*. 2008, 46(2).
- Wu Z, Huang N E. Ensemble empirical mode decomposition: a noise-assisted data analysis method[J]. *Advances in adaptive data analysis*. 2009, 1(01): 1-41.
- Xie, X., Zaitsev, Y., Velásquez-García, L. F., Teller, S. J., & Livermore, C. (2014). Scalable,

- MEMS-enabled, vibrational tactile actuators for high resolution tactile displays. *Journal of Micromechanics and Microengineering*, 24(12), 125014.
- Yang, C., Liu, S., Xie, X., & Livermore, C. (2016). Compact, planar, translational piezoelectric bimorph actuator with Archimedes' spiral actuating tethers. *Journal of Micromechanics and Microengineering*, 26(12), 124005.
- Xie, X., & Livermore, C. (2017, January). Passively self-aligned assembly of compact barrel hinges for high-performance, out-of-plane mems actuators. In *Micro Electro Mechanical Systems (MEMS), 2017 IEEE 30th International Conference on* (pp. 813-816). IEEE.
- Xie, X., & Livermore, C. (2016, January). A pivot-hinged, multilayer SU-8 micro motion amplifier assembled by a self-aligned approach. In *Micro Electro Mechanical Systems (MEMS), 2016 IEEE 29th International Conference on* (pp. 75-78). IEEE.
- Xie, X., & Livermore, C. (2015). A high-force, out-of-plane actuator with a MEMS-enabled microscissor motion amplifier. In *Journal of Physics: Conference Series* (Vol. 660, No. 1, p. 012026). IOP Publishing.
- Yang, C., Xie, X., Liu, S., & Livermore, C (2017, June). Resealable, ultra-low leak micro valve using liquid surface tension sealing for vacuum applications. In *Solid-State Sensors, Actuators and Microsystems (TRANSDUCERS), 2017 Transducers-2017 19th International Conference on* (pp. 2071-2074). IEEE.
- Xie, X., Zaitsev, Y., Velasquez-Garcia, L., Teller, S., & Livermore, C. (2014). Compact, scalable, high-resolution, MEMS-enabled tactile displays. In *Proc. of Solid-State Sensors, Actuators, and Microsystems Workshop* (pp. 127-130).
- Xu, J., Xie, X., Yang, C., Shen, Z. (2017), Test and Analysis of Hydraulic Fracture Characteristics of Rock Single Crack. *Fluid Mech Open Acc* 4: 164. doi: 10.4172/2476-2296.1000164
- Xie, Xin. "High Performance Micro Actuators for Tactile Displays." Order No. 10273384 Northeastern University, 2017. Ann Arbor: ProQuest. Web. 17 Aug. 2017.
- Livermore-Clifford, C., Xie, X., Teller, S. and Velasquez-garcia, L., Northeastern University, 2015. Devices, methods, and systems for high-resolution tactile displays. U.S. Patent Application 14/589,732.
- Jake Roemer, Mark Groman, Zhengyu Yang, Yufeng Wang, Chiu C. Tan, and Ningfang Mi, "Improving Virtual Machine Migration via Deduplication", 11th IEEE International Conference on Mobile Ad Hoc and Sensor Systems (MASS 2014), 2014.
- Jianzhe Tai, Deng Liu, Zhengyu Yang, Xiaoyun Zhu, Jack Lo, and Ningfang Mi, "Improving Flash Resource Utilization at Minimal Management Cost in Virtualized Flash-based Storage Systems", *IEEE Transactions on Cloud Computing*, 2015.
- Zhengyu Yang, Manu Awasthi, Mrinmoy Ghosh, and Ningfang Mi, "A Fresh Perspective on Total Cost of Ownership Models for Flash Storage in Datacenters", 8th IEEE International Conference on Cloud Computing Technology and Science (CloudCom 2016), 2016.
- Zhengyu Yang, Jianzhe Tai, Janki Bhimani, Jiayin Wang, Ningfang Mi, and Bo Sheng, "GREM: Dynamic SSD Resource Allocation in Virtualized Storage Systems with Heterogeneous IO Workloads", 35th IEEE International Performance Computing and Communications Conference (IPCCC 2016), 2016.
- Jiayin Wang, Teng Wang, Zhengyu Yang, Ningfang Mi, and Bo Sheng, "eSplash: Efficient Speculation in Large Scale Heterogeneous Computing Systems", 35th IEEE International

- Performance Computing and Communications Conference (IPCCC 2016), 2016.
- Janki Bhimani, Jingpei Yang, Zhengyu Yang, Ningfang Mi, Qiumin Xu, Manu Awasthi, Rajinikanth Pandurangan, and Vijay Balakrishnan, "Understanding Performance of I/O Intensive Containerized Applications for NVMe SSDs", 35th IEEE International Performance Computing and Communications Conference (IPCCC 2016), 2016.
- Zhengyu Yang, Jiayin Wang, David Evans, and Ningfang Mi, "AutoReplica: Automatic Data Replica Manager in Distributed Caching and Data Processing Systems", 1st IEEE International Workshop on Communication, Computing, and Networking in Cyber Physical Systems (CCNCPS 2016), 2016.
- Jiayin Wang, Teng Wang, Zhengyu Yang, Ying Mao, Ningfang Mi, and Bo Sheng, "SEINA: A Stealthy and Effective Internal Attack in Hadoop Systems", International Conference on Computing, Networking and Communications (ICNC 2017), 2017.
- Han Gao, Zhengyu Yang, Janki Bhimani, Teng Wang, Jiayin Wang, Bo Sheng, and Ningfang Mi, "AutoPath: Harnessing Parallel Execution Paths for Efficient Resource Allocation in Multi-Stage Big Data Frameworks", 26th International Conference on Computer Communications and Networks (ICCCN 2017), 2017.
- Teng Wang, Jiayin Wang, Nam Nguyen, Zhengyu Yang, Ningfang Mi, and Bo Sheng, "EA2S2: An Efficient Application-Aware Storage System for Big Data Processing in Heterogeneous Clusters", 26th International Conference on Computer Communications and Networks (ICCCN 2017), 2017.
- Janki Bhimani, Ningfang Mi, Miriam Leeser, and Zhengyu Yang, "FiM: Performance Prediction Model for Parallel Computation in Iterative Data Processing Applications", 10th IEEE International Conference on Cloud Computing (CLOUD 2017), 2017.
- Janki Bhimani, Zhengyu Yang, Miriam Leeser, and Ningfang Mi, "Accelerating Big Data Applications Using Lightweight Virtualization Framework on Enterprise Cloud", 21st IEEE High Performance Extreme Computing Conference (HPEC 2017), 2017.
- Zhengyu Yang, Mrinmoy Ghosh, Manu Awasthi, Vijay Balakrishnan, "Online Flash Resource Allocation Manager Based on TCO Model", US15/092156, US20170046089A1, 2016.
- Zhengyu Yang, Mrinmoy Ghosh, Manu Awasthi, Vijay Balakrishnan, "Online Flash Resource Migration, Allocation, Retire and Replacement Manager Based on a Cost of Ownership Model", US15/094971, US20170046098A1, 2016.
- Zhengyu Yang, Sina Hassani, and Manu Awasthi, "Memory Device Having a Translation Layer with Multiple Associative Sectors", US15/093682, 2016.
- Zhengyu Yang and Manu Awasthi, "I/O Workload Scheduling Manager for RAID/non-RAID Flash Based Storage Systems for TCO and WAF Optimizations", US15/396186, 2017.
- Zhengyu Yang, Jiayin Wang, and David Evans, "Adaptive Caching Replacement Manager with Dynamic Updating Granulates and Partitions for Shared Flash-Based Storage System", US15/400835, 2017.
- Zhengyu Yang, Jiayin Wang, and David Evans, "A Duplicate In-memory Shared-intermediate Data Detection and Reuse Module in Spark Framework", US15/404100, 2017.
- Zhengyu Yang, Jiayin Wang, and David Evans, "Automatic Data Replica Manager in Distributed Caching and Data Processing Systems", US15/408328, 2017.
- Jiayin Wang, Zhengyu Yang, and David Evans, "Efficient Data Caching Management in Scalable Multi-stage Data Processing Systems", US15/423384, 2017.

- Xie, X., Liu, S., Yang, C., Yang, Z., Xu, J., & Zhai, X. (2017). The application of smart materials in tactile actuators for tactile information delivery. arXiv preprint arXiv:1708.07077.
- Juncai Xu, Zhenzhong Shen, Song Yang, Xin Xie, Zhengyu Yang, Finite Element simulation of Prevention Thermal Cracking in Mass Concrete, Int. J. of Computing Science and Mathematics, 2017
- Juncai Xu, Zhenzhong Shen, Qingwen Ren, Xin Xie, Zhengyu Yang, Slope Stability Analysis with Geometric Semantic Genetic Programming. arXiv preprint arXiv: 1708.09116 (2017).
- Juncai Xu, Qingwen Ren, Zhenzhong Shen, Xin Xie, Zhengyu Yang, Xianglin Zhai, Prediction Method for Concrete Carbonation Depth Based on Extreme Learning Machine, arXiv. 2017
- Tian Liu, Sanwei Liu, Xin Xie, Chenye Yang, Zhengyu Yang, Xianglin Zhai, Smart materials and structures for energy harvesters, arXiv: 1709.00493
- Qinghai Jiang, Kai Wu, Yu Sun, Xin Xie, Zhengyu Yang, A Discrete Packing Model of Granular Material Confined in A Vertical Column, arXiv: 1709.01001
- Juncai Xu, Weidong Zhang, Qingwen Ren, Xin Xie, and Zhengyu Yang, SSE Lossless Compression Method for the Text of the Insignificance of the Lines Order, arXiv:1709.04035
- Juncai Xu, Zhenzhong Shen, Qingwen Ren, Xin Xie, Zhengyu Yang, Geometric Semantic Genetic Programming Algorithm and Slump Prediction, arXiv:1709.06114
- Colominas M A, Schlotthauer G, Torres M E. Improved complete ensemble EMD: A suitable tool for biomedical signal processing[J]. Biomedical Signal Processing & Control. 2014, 14(1): 19-29.
- Chen W. Ground roll attenuation using improved complete ensemble empirical mode decomposition[J]. Journal of Seismic Exploration. 2016, 25(5).